Journal of Wind Engineering and Industrial Aerodynamics, 24 (1986) 215—225
Elsevier Science Publishers B.V., Amsterdam — Printed in The Netherlands

MULTIPLE ACTUATOR-DISC THEORY FOR WIND TURBINES

B.G. NEWMAN

Department of Mechanical Engineering, McGill University, Montreal, PQ (Canada)

(Received November 11, 1985; accepted in revised form February 24, 1986)

Summary

If the effects of fluid rotation are neglected, one-dimensional theory for a single actuator disc gives a maximum power coefficient of 16/27. This is the usual Betz limit for the power of horizontal-axis wind turbines.

Tandem discs are a more appropriate representation for a vertical-axis, Darrieus, wind turbine and give more accurate predictions of turbine performance when used in conjunction with blade element theory. The maximum power coefficient for two discs in tandem is 16/25.

In the present paper the case of n actuator discs is considered. It is shown that the maximum power coefficient is $[8n(n+1)]/[3(2n+1)^2]$. The corresponding axial inflow factor for the rth disc is $(2r-1)/(2r+1)$, and the outflow factor for the outer annulus of that disc is $2r/(2r+1)$. For a very large number of discs the maximum power coefficient is thus 2/3, which is 13% larger than the maximum for a single disc.

Some flow visualization experiments on flow through tandem screens are presented which indicate that the minimum spacing below which the theory begins to become inaccurate is about one half of a disc diameter.

Notation

a	Axial inflow factor
A_{mr}	Area of the particular annular streamtube as it crosses disc m to eventually become the outer streamtube for disc r
b	Axial outflow factor
C_P	Total power coefficient (sometimes called the efficiency of a wind turbine)
C_{P_r}	Power coefficient for the rth disc
K	Local pressure drop coefficient across a disc $\dfrac{p-q}{\frac{1}{2}\rho V^2(1-a)^2}$
n	Total number of discs
p	Pressure just upwind of a disc
p	Ambient pressure
q	Pressure just downwind of a disc
Q_r	Volume flux in the outer annular streamtube of disc r

0167-6105/86/$03.50

Re	Reynolds number based on velocity normal to a screen
S_r, S_m, S_n	Series identified in the appendix
V	Wind speed
ρ	Air density

Suffices

m	mth disc
r	rth disc
n	total number of discs

1. Introduction

The purpose of this paper is to extend the classical theory of Betz [1] for the maximum power output of a wind turbine. In this theory the turbine, usually of the horizontal-axis or propeller type, is replaced by a single actuator disc through which the flow is assumed to be one dimensional: the maximum power coefficient is 0.59 (Glauert [2]). For vertical-axis wind turbines of the Darrieus type (Templin [3]) tandem discs are a more appropriate representation (Lapin [4]; Robert [5]; Paraschivoiu and Delclaux [6]) and for two discs the maximum power coefficient is 0.64 (Newman [7]). The extension in the present paper (Newman [8]) is to n actuator discs and has already been considered in a simpler way by Loth and McCoy [9]. The analysis in this paper is also compared with some flow visualization experiments in a smoke tunnel.

2. Theory

Consider a wind turbine which is represented by n actuator discs. The spacing between the discs is sufficient that the flow through each disc may be taken as one dimensional. In Fig. 1 the velocity on either side of the rth disc is constant and equal to $V(1-a_r)$. The outer streamtube for this disc which just bypasses the $(r+1)$th disc has an outflow factor b_r and hence an annular wake velocity of $V(1-b_r)$. The pressures upstream and downstream of the rth disc are denoted by p_r and q_r, respectively.

The areas of the various streamtubes as they cross each disc are identified

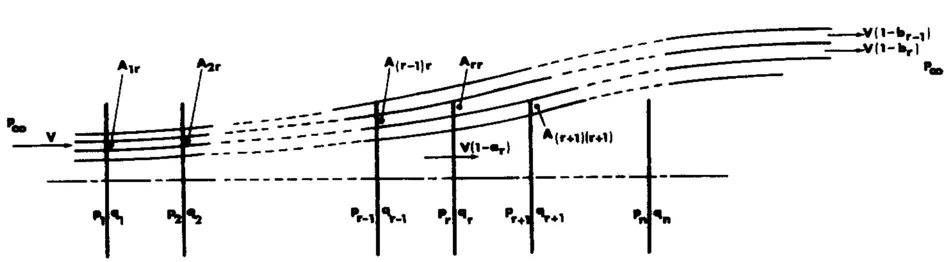

Fig. 1. The streamlines through n actuator discs.

as A_{mr} where m identifies the disc, and r the particular streamtube which eventually becomes the outer one for the rth disc, as shown in Fig. 1.

Consider the complete annular streamtube which is the outer streamtube of the rth disc and choose it as a control volume for momentum in the axial direction. As in the previous paper [7] the longitudinal force due to the pressures acting on the curved boundaries of each annular control volume is neglected. This can be justified for the outer edge of the slipstream for a single disc (Milne-Thomson [10]) but is difficult to justify generally. However the assumption is customarily adopted for both single actuator disc theory with rotation (Betz [1]) and blade element theory with small inflow [10,11].

$$(p_1-q_1)A_{1r}+(p_2-q_2)A_{2r}+\ldots+(p_r-q_r)A_{rr} = \rho Q_r V b_r$$

where Q_r = volume flow in the streamtube

$$= V(1-a_1)A_{1r} = V(1-a_2)A_{2r} = \ldots = V(1-a_r)A_{rr}$$

$$\text{Thus } \frac{p_1-q_1}{1-a_1}+\frac{p_2-q_2}{1-a_2}+\ldots+\frac{p_r-q_r}{1-a_r} = \rho V^2 b_r$$

$$\text{It follows that } \frac{p_r-q_r}{1-a_r} = \rho V^2(b_r-b_{r-1}) \tag{1}$$

Bernoulli's equation is now applied upstream and downstream of the discs.

downstream of disc r: $\quad p_\infty + \tfrac{1}{2}\rho V^2(1-b_r)^2 = q_r + \tfrac{1}{2}\rho V^2(1-a_r)^2$

downstream of disc $(r-1)$: $\quad p_\infty + \tfrac{1}{2}\rho V^2(1-b_{r-1})^2 = q_{r-1} + \tfrac{1}{2}\rho V^2(1-a_{r-1})^2$

between discs $(r-1)$ and r: $\quad q_{r-1} + \tfrac{1}{2}\rho V^2(1-a_{r-1})^2 = p_r + \tfrac{1}{2}\rho V^2(1-a_r)^2$

$$\text{Thus } p_r-q_r = \tfrac{1}{2}\rho V^2[(1-b_{r-1})^2-(1-b_r)^2]$$

$$= \tfrac{1}{2}\rho V^2[b_r-b_{r-1}][2-b_{r-1}-b_r] \tag{2}$$

Comparing eqns. (1) and (2), $b_r + b_{r-1} = 2a_r$ for all discs (3)
(Note that if $r = n = 1$, $b_1 = 2a_1$, the usual result.)

By successively applying the recursion equation (3)

$$b_r = 2(a_r - a_{r-1} + a_{r-2} + \ldots + (-1)^{r-2}a_2 + (-1)^{r-1}a_1) \tag{4}$$

The power coefficient for the complete system of discs

$$C_P = \sum_{r=1}^{r=n} \frac{(p_r-q_r)AV(1-a_r)}{\tfrac{1}{2}\rho AV^3}$$

where A is the total area of each disc.

$$\frac{C_P}{4} = \sum_{r=1}^{r=n}(a_r-2a_{r-1}+2a_{r-2}+\ldots+(-1)^{r-1}2a_1)(1-a_r)^2 \tag{5}$$

in which it is understood $a_m = 0$ when $m < 1$.

If C_P is a maximum, $\frac{1}{4}\frac{\partial C_P}{\partial a_r} = 0$ for all integer values of r between 1 and n. Thus

$$(1-a_r)^2 - 2(1-a_r)(a_r - 2a_{r-1} + 2a_{r-2} + \ldots + (-1)^{r-1}\, 2a_1)$$
$$+ 2(-(1-a_{r+1})^2 + (1-a_{r+2})^2 + \ldots + (-1)^{n-r}(1-a_n)^2) = 0 \qquad (6)$$

for all values of r between 1 and n.

The solution for 1 and 2 discs is known. The solution for 3 discs is also fairly easy to work out. These values of a_r are shown in Table 1.

TABLE 1

Optimum values of a_r

n	r		
	1	2	3
1	1/3	—	—
2	1/5	3/5	—
3	1/7	3/7	5/7

The sequence of numbers suggests trying

$$a_r = \frac{2r-1}{2n+1} \qquad (7)$$

as the general solution for eqn. (6). The left hand side is

$$\left[\frac{2}{(2n+1)}\right]^2 \left\{(n-r+1)^2 - (n-r+1)\left((2r-1) - 2(2r-3) + 2(2r-5) \ldots 2(-1)^{r-1}\right.\right.$$
$$\left.\left. + 2 - (n-r)^2 + (n-r-1)^2 - (n-r-2)^2 + \ldots + (-1)^{n-r}\right)\right\}$$
$$= \left[\frac{2}{(2n+1)}\right]^2 \left\{(n-r+1)\,(n-r+1 - 2r - (2r-1)) - 2\,\frac{(n-r)(n-r+1)}{2}\right\}$$

by quoting the series S_r and S_m which are given in the appendix the above expression equals zero which checks.

The associated value of b_r is, from eqn. (4)

$$b_r = \frac{2}{2n+1}\ \{(2r-1) - (2r-3) + (2r-5) + \ldots + (-1)^{r-1}\}$$
$$= \frac{2r}{2n+1} \qquad (8)$$

The corresponding value of C_P is, from eqn. (5)

$$C_P = \frac{4}{(2n+1)^3} \sum_{r=1}^{r=n} \{-(2r-1) + 2r\}\, 2(n-r+1)^2$$

$$= \frac{16}{(2n+1)^3} \, \frac{n(n+1)(2n+1)}{6}$$

from series S_n in the appendix

$$= \frac{8n(n+1)}{3(2n+1)^2} \qquad (10)$$

For $n = 1$, $C_P = 16/27$ and for $n = 2$, $C_P = 16/25$.

Both these values have been shown to be maxima [1,7], so it may be assumed that eqn. (10) also gives the maximum value for n discs.

The values of $C_{P_{max}}$ are plotted against the number of discs in Fig. 2. The limiting value for n large is 2/3 and is seen to be close to this value when $n = 4$.

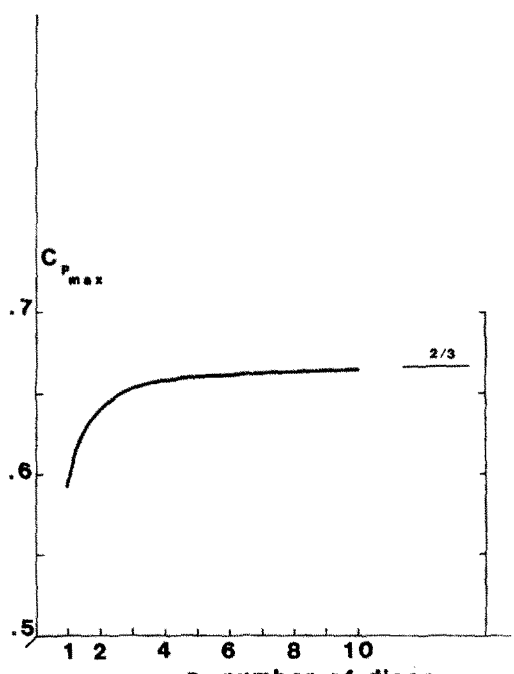

Fig. 2. The maximum power coefficient as a function of the number of discs.

The power "absorbed" separately by the rth disc, when conditions are optimum, is

$$C_{P_r} = \frac{(p_r - q_r)\,A\,V(1-a_r)}{\tfrac{1}{2}\rho A V^3}$$

From eqn. (5)

$$C_{P_r} = \frac{16(n-r+1)^2}{(2n+1)^3} \tag{11}$$

Table 2 shows that most of the power is absorbed by the upwind disc(s) and that the gain from increasing the number of discs from 2 to 4 may be outweighed by the increased cost of the machine. A possible vertical-axis wind turbine with 4 discs might consist of two, two-bladed rotors of significantly different diameter, running on concentric shafts and perhaps rotating in opposite directions.

TABLE 2

Contribution to the power from each disc

r	(n=4) C_{P_r}	(n=2) C_{P_r}	(n=1) C_{P_r}
1	0.351	0.512	0.593
2	0.198	0.128	
3	0.088		
4	0.022		
Total	0.658	0.640	0.593

3. The effect of disc spacing

It has been assumed that the flow through each disc is one dimensional and the final results are independent of disc spacing. For very large spacing the static pressure between each disc will be atmospheric: indeed Loth and McCoy [9] obtained the present results by assuming that the flow is vented between each disc. As the discs are moved closer together this particular assumption will become incorrect and the flow pattern will resemble Fig. 1 of this paper rather than Fig. 1 of ref. 9. Eventually even the assumptions of one-dimensional flow will become invalid. Taylor [12] examined this question for a single disc by replacing it with an array of sources which represented the displacement effect associated with the drag of each element of the disc (which in his case represented a very porous screen). In this way the flow ahead of the screen could be calculated and the degree of pressure variation assessed in terms of the curvature of the upstream streamlines. In the present case this type of analysis could be attempted numerically for an array of discs, but it seemed simpler in the case of a few discs to set up a smoke tunnel experiment to visualize the flow for various disc spacings and also to set up the optimum single disc for comparison. The actuator discs are approximately represented by very porous screens, the characteristics of which are usually expressed in terms of a parameter

$$K = \frac{\text{pressure drop}}{\text{local dynamic pressure}}$$

For the rth disc of an array of n discs

$$K_r = \frac{p_r - q_r}{\tfrac{1}{2}\rho V^2 (1-a_r)^2}$$

$$= \frac{(b_r - b_{r-1})(2 - b_{r-1} - b_r)}{(1-a_r)^2}$$

$$= \frac{2}{n-r+1} \quad \text{for the optimum condition.}$$

For $n = 1$, $K = 2$.

For $n = 2$, the upstream disc $K = 1$ and the downstream disc $K = 2$.

The local velocities and the ideal powers for the tandem discs $n = 2$ are shown in Fig. 3.

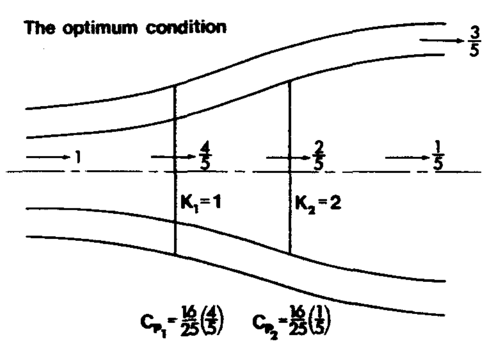

Fig. 3. The optimum condition for two discs.

Special precautions had to be taken in setting up the experiment, which were based on experience with earlier set-ups.

(1) The K of a screen is not constant at the low speeds which are used in a smoke tunnel: K increases with decreasing Reynolds number; K was measured for a range of Reynolds numbers based on the screen diameter for a variety of screens. It was possible to select two which would give the

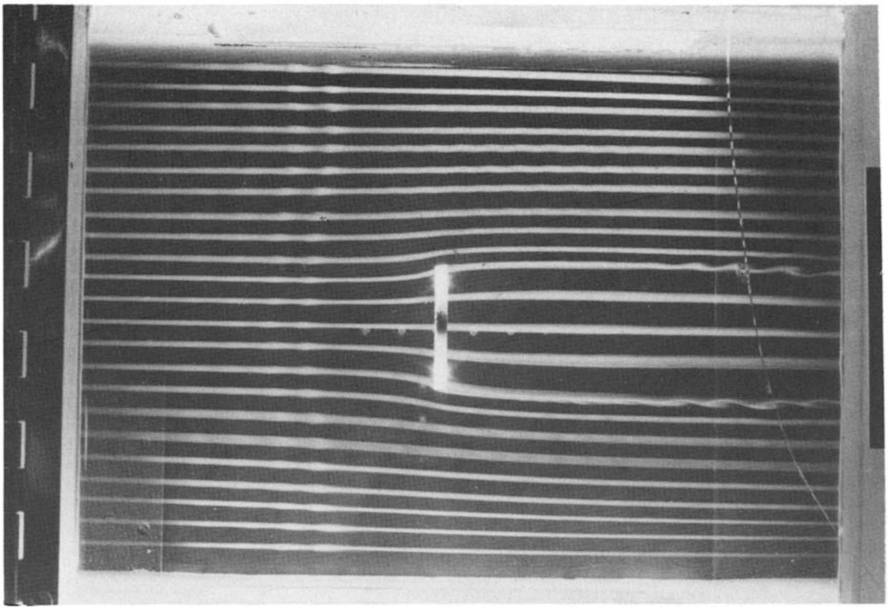

Fig. 4. Smoke tunnel picture for a single disc with $K = 2$: flow from left to right.

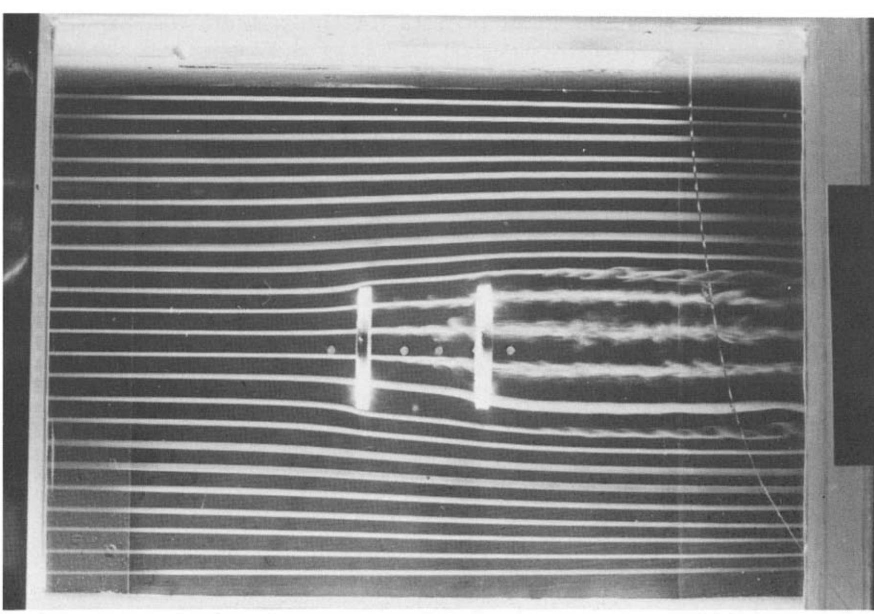

Fig. 5. Smoke tunnel picture: double disc with conditions corresponding to Fig. 3 spacing/diameter = 1.00.

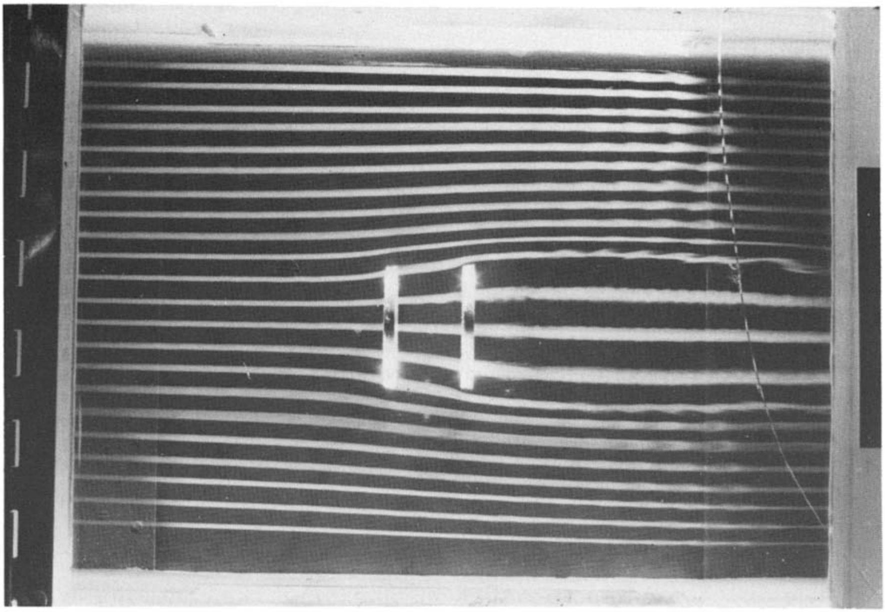

Fig. 6. Smoke tunnel picture: double disc with spacing/diameter = 0.66.

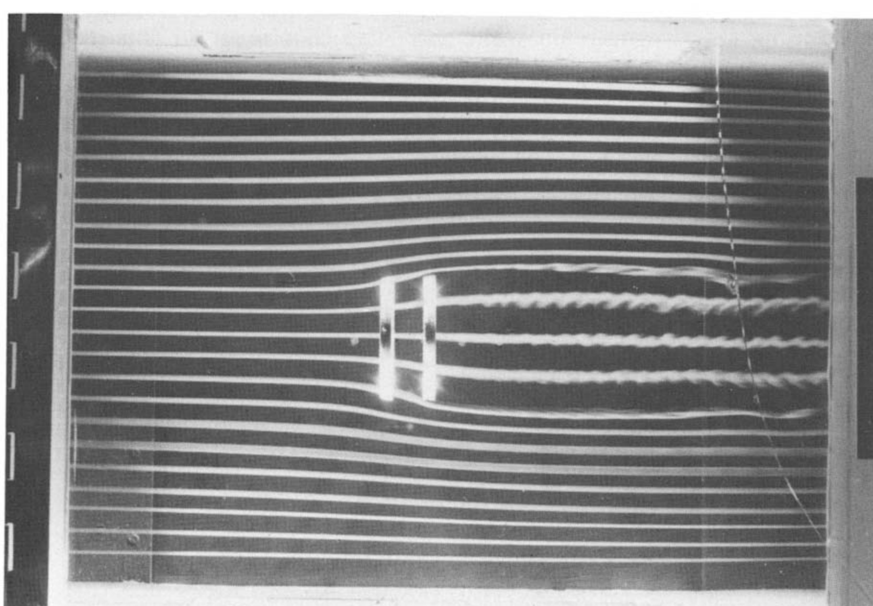

Fig. 7. Smoke tunnel picture: double disc with spacing/diameter = 0.33.

TABLE 3

Characteristics of the chosen screen

Screen	Spacing	Diameter	K	at	Re
Fused plastic flyscreen	1.7 mm	0.35 mm	2		24.4
Woven plastic netting	1.2 mm	0.19 mm nominal	1		26.3

required values of K for a particular speed of the smoke tunnel. Theoretical values were used to correlate the speeds through each screen. The chosen screens are listed in Table 3.

The values of K are probably accurate to ± 0.02.

(2) The screens were mounted on rings of diameter 25.4 mm which were made slightly conical (included angle 10°) in order to minimize the wake produced by the rings. The cross section of the smoke tunnel was 88.9 mm × 177.8 mm.

For a single disc $K = 2$ the streamline spacing about the centerline when squared gives the velocity ratios 2/3 at the disc and 1/3 far downstream. These are the values of $1-a_r$ and $1-b_r$ in eqns. (7) and (8) when $r = n = 1$. For the pictures shown in Fig. 4 the spacing is in agreement at the disc but far downstream the value is 0.44 instead of 0.33. A simple analysis of the flow surrounding the downstream wake indicates that most of this discrepancy is due to tunnel blockage.

For the double discs with a spacing of d and $0.67d$ agreement is again very good at both discs but is 0.3 to 0.35 instead of 0.2 far downstream. For a closer spacing of $0.33d$ there is significant disagreement at the discs themselves, indeed the upstream spacing tends towards a value similar to that for a single disc.

It is concluded that the present theory begins to become inaccurate due to curvature of the streamlines at the disc and lack of flow uniformity when the disc spacing is less than about $0.5d$.

4. Conclusions

(1) The maximum "power" of a wind turbine represented by an array of n discs is $\dfrac{8n(n+1)}{3(2n+1)^2}$. For large n (effectively $n > 6$) the optimum value is therefore 2/3 compared with the Betz value of 16/27 for $n = 1$.

(2) The corresponding of values for the rth disc in the array are: for the inflow factor $a_r = \dfrac{2r-1}{2n+1}$ and for the outflow factor $b_r = \dfrac{2r}{2n+1}$.

(3) The minimum spacing below which this one-dimensional theory begins

to fail is approximately $0.5d$. A two-disc model of a Darrieus wind turbine is therefore usually satisfactory.

(4) The present theory gives optimum values of the inflow factor at each disc which might be used to improve the design of Darrieus wind turbines. Since most of the power should be absorbed by the upwind disc(s) cambered, or alternatively canted, aerofoils might be used to advantage.

Acknowledgement

The K/Re characteristics of the screens were measured by Mr. Anthony Sharp.

Appendix

Three series are used in the present analysis

$$S_r = (2r-1) - (2r-3) + (2r-5) + \ldots + (-1)^{r-1} = r$$

$$S_m = m^2 - (m-1)^2 + (m-2)^2 - (m-3)^2 + \ldots + (-1)^{m-1} = \frac{m(m+1)}{2}$$

$$S_n = n^2 + (n-1)^2 + (n-2)^2 + \ldots + 1^2 = \frac{n(n+1)(2n+1)}{6}$$

References

1 A. Betz, Eine Erweiterung der Schraubenstrahl-Theorie, Z. Flugtechnik Motorl., 11 (1920) 105—110.

2 H. Glauert, in W.F. Durand (Ed.), Windmills and Fans, Aerodynamic Theory, Vol. 4, Springer, Berlin, 1935, p. 327.

3 R.J. Templin, Aerodynamic performance theory for the N.R.C. vertical-axis wind turbine, N.R.C. Canada Rep. LTR-LA-160, 1974.

4 E.E. Lapin, Theoretical performance of vertical axis wind machines, ASME Paper 75-WA/ENER 1, Houston, TX, 1975.

5 J. Robert, Sail aerofoil applied to a vertical-axis wind turbine, M. Eng. thesis, McGill University, Montreal, 1977.

6 I. Paraschivoiu and F. Delclaux, Double multiple streamtube model with recent improvements, AIAA J. Energy, 7 (1983) 250—255.

7 B.G. Newman, Actuator disc theory for vertical-axis wind turbines, J. Wind Eng. Ind. Aerodyn., 15 (1983) 347—355.

8 B.G. Newman, Multiple actuator-disc theory for wind turbines, 16th Int. Cong. of Theor. and Appl. Mech., Lyngby, Denmark, Pap. 145, 1984.

9 J.L. Loth and H. McCoy. Optimization of Darrieus turbines with an upwind and downwind momentum model, AIAA J. Energy, 7 (1983) 313—318.

10 L.M. Milne-Thomson, Theoretical Aerodynamics, MacMillan, New York, 1958, p. 240.

11 H. Glauert, The Elements of Aerofoil and Airscrew Theory, 2nd edn., Cambridge University Press, 1947, pp. 210, 211.

12 G.I. Taylor, Air resistance of a flat plate of very porous material, A.R.C., R & M 2236 (1944).